



## Hippocampus Segmentation Based On Priori Shape Model with Region Growing From High-Resolution MRI of Post-Mortem Samples

K.Somasundaram\* and S.Vijayalakshmi

Image Processing Lab

Department of Computer Science and Applications

Gandhigram Rural Institute-Deemed University

Gandhigram, Dindigul, Tamil Nadu, 624 302, India.

somasundaramk@yahoo.com\*, sviji\_suji@yahoo.co.in

**Abstract:** This paper describes a simple method for segmenting the hippocampus automatically from high-resolution 9.4 Tesla MRI of postmortem samples. Large datasets of high-resolution structural MR images are collected to quantitatively analyze the relationships between brain anatomy, disease progression, treatment regimens, and genetic influences upon brain structure. This method segments the hippocampus without any human intervention for few slices present in the anterior and the posterior position in the total volume. Experimental results using this method show a good agreement with the manuals segmented gold standard.

**Keywords:** Hippocampus; amygdala; post-mortem; Alzheimer's disease; neuropathology; morphometry; cornu ammonis; dentate gyrus

### I. INTRODUCTION

Hippocampus in the human brain plays a vital role in the functionality of the brain. It's primary function is related with encoding of episodic memory. It is involved in the encoding and retrieval of other types of long term memory. Hippocampal neuropathology is important in the study of dementia, epilepsy, schizophrenia and other neurological and psychiatric disorders. However, the complex anatomy of the hippocampus poses challenges to image-based computational morphometric techniques. The hippocampus is formed by two interlocking folded layers of neurons, the cornu ammonis (CA) and the dentate gyrus (DG). It is very difficult to distinguish the boundaries between hippocampal layers in clinical magnetic resonance image (MRI) modalities, since the voxel resolution of  $\approx 1$  mm<sup>3</sup> (isotropic) is larger than the thickness of the DG. So a high-resolution 9.4 Tesla MRI of postmortem samples are used in our study. Hence, a simple approach has been made to segment hippocampus at least in few slices.

In [1], a technique for automatically assigning a neuroanatomical label to each voxel in an MRI volume, based on probabilistic information automatically estimated from a manually labeled training set, was proposed. In contrast to existing segmentation procedures that label a small number of tissue classes, this method assigns one of 37 labels to each voxel, including left and right caudate, putamen, pallidum, thalamus, lateral ventricles, hippocampus, and amygdala. The classification technique employs a registration procedure that is robust to anatomical variability, including the ventricular enlargement typically associated with neurological diseases and aging. In [2], a novel method has been proposed for localization of the hippocampus. In their study they used landmark localization, a statistical roadmap and anatomical landmarks, to reach the desired structures. These landmarks were identified using a training set for artificial neural network (ANN). They estimated a Gaussian model and determined the optimal search areas for desired landmarks.

In [3] a computational atlas of the human hippocampus from postmortem magnetic resonance imaging at 9.4 Tesla was provided. They have also provided subfield segmentation in the hippocampus. In [4], a comparative study of the performance of two popular and fully automated tools, FSL/FIRST and FreeSurfer with that of the manual tracing, for quantifying hippocampal and amygdala volume has been reported. This study helps to understand the shape of hippocampus. In their method they have computed the volume overlap, volume difference, across-sample correlation and 3-D group-level shape analysis. In addition, sample size estimates for conducting between-group studies were computed for a range of effect sizes. In [5], Fully deformable registration methods, cohort atlases, and user-defined manual tracings are discussed. In [6], functional anatomy was discussed. In [7] High dimensional diffeomorphic transformations of a neuroanatomical template, hippocampal volume and surfaces are used. In [8-10], hippocampal subfields were analysed.

In this paper we present an automated tool to segment the hippocampus from high-resolution, 9.4 Tesla, MRI of postmortem samples. Our method segments the hippocampus in few slices of the entire volume. The remaining part of the paper is organized as follows. In section II, we present the methods and the materials. In section III, the results and discussion are given. Finally in section IV, the conclusion is given.

### II. MATERIALS AND METHODS

#### A. Materials Used:

The materials used for this work are obtained from the Penn Hippocampus Atlas [3] (PHA). PHA is a resource consisting of segmented and normalized high-resolution postmortem MRI of the human hippocampus. The atlas is described by Yushkevich et al[3].

**B. Methods:**

The proposed method is a generalized method for segmenting the hippocampus in the left side of the brain for the slices from Penn002L\_01070 to Penn002L\_01100. The flow chart of the proposed method is shown in Fig.1. It consists of two stages. In the first stage a priori shape model is constructed by analyzing the manually segmented results available in PHA. This priori shape model is a common region formed by the intersection between the manually segmented hippocampus for the slices from Penn002L\_01070 to Penn002L\_01100. If  $A_i$  is the manually segmented hippocampus of the  $i^{th}$  slice, the priori shape model A for the

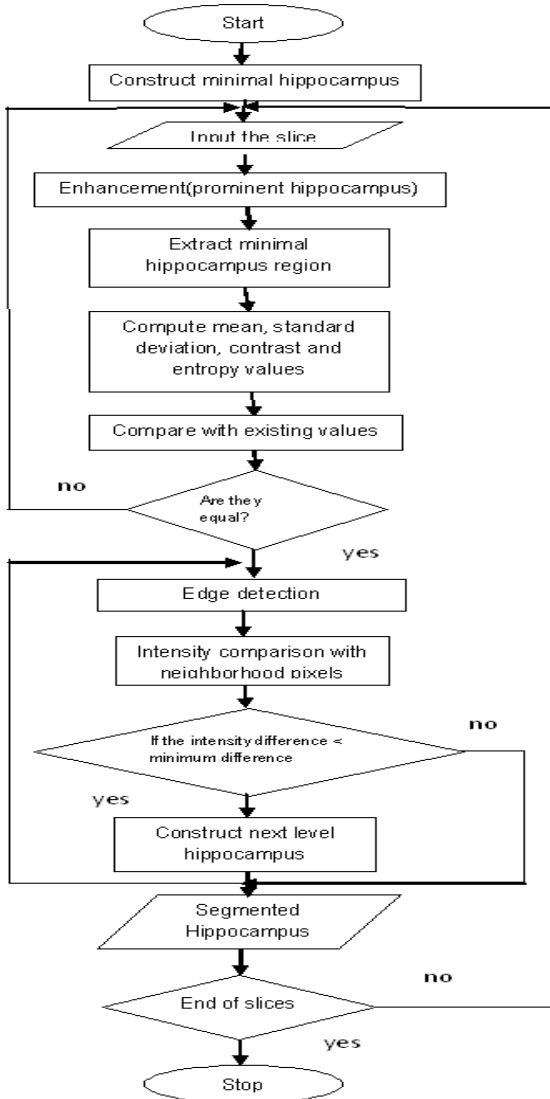


Figure. 1. Flowchart of proposed method slices 1 to n (here the i value ranges from 70 to 100) is given by

$$A = \bigcap_{i=1}^n A_i \tag{1}$$

The priori shape model for the left hippocampus for the slices from Penn002L\_01070 to Penn002L\_01100 thus obtained by the above process is shown in Fig.2(a). Any input slice (one among the slices from Penn002L\_01070 to Penn002L\_01100) is of the form shown in Fig 2(b). The priori shape modal can be superimposed on the original slice as shown in Fig 2(c), to test whether a signature of the priori shape is available on the image.

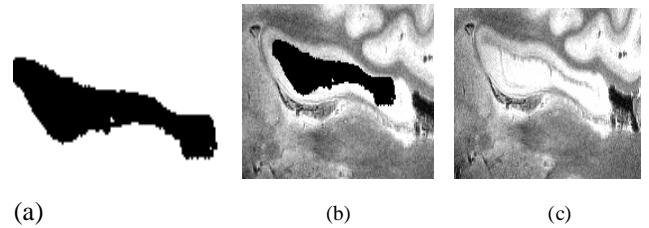


Figure.2. (a) Priori shape model (b) Input image (c) Priori shape model superimposed on input image

If the input slice is one among the slices from Penn002L\_01070 to Penn002L\_01100 then it should contain the priori shape in the above said position (Fig.2(c)), which has been calculated from the analysis of manually segmented results available in PHA. So, the proposed method extracts this specific region (hereafter referred as minimal hippocampus) from the input slice and then analyses whether the extracted portion is hippocampus or not using the features such as mean, standard deviation, entropy and contrast.

The mean value T of the minimal hippocampus is computed as :

$$T = \frac{\sum_{x=1}^m \sum_{y=1}^n f(x,y)}{m \times n} \tag{2}$$

Where  $f(x,y)$  is the intensity of the pixel  $A(i,j)$ , m is the number of rows and n is the number of columns. The standard deviation of the minimal hippocampus is computed as :

$$S = \left( \frac{1}{n} \sum_{i=1}^n (x_i - \bar{x})^2 \right)^{1/2} \tag{3}$$

where ,

$$\bar{x} = 1/n \sum_{i=1}^n x_i \tag{4}$$

Where  $x_i$  is the intensity of the pixel at  $i^{th}$  position.

Entropy is a statistical measure of randomness that can be used to characterize the texture of the input image. Entropy E of the minimal hippocampus is defined as

$$E = \text{sum}(p \cdot \log_2(p)) \tag{5}$$

Where p is the histogram counts.

Contrast is a measure of the intensity contrast between a pixel and its neighbor over the whole image. The contrast C of the minimal hippocampus is given by:

$$C = \sum_{i,j} |i - j|^2 p(i,j) \tag{6}$$

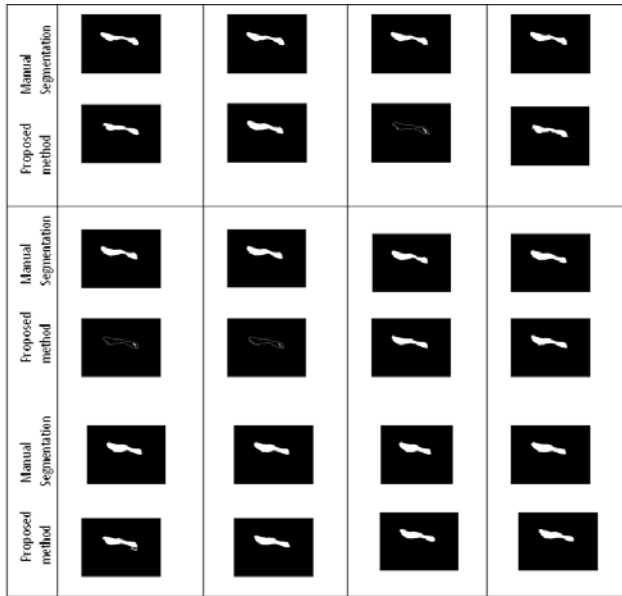
where,  $p(i,j)$  is the intensity of pixel at  $(i,j)^{th}$  position.

The range of values of the above said features for the minimal hippocampus are derived from the manually segmented images available in PHA and are given in Table1.

Table 1. Features of manually segmented Hippocampus

Feature	Value	
	Minimum	Maximum
Mean ( $\bar{x}$ )	218	235
Standard deviation ( $\sigma$ )	5.4	7.5
Entropy (E)	0.23	0.26
Contrast (C)	0.0014	0.0154

In the second stage the test slices are taken for segmentation. For the input slice, the values of the features  $\bar{x}$ ,  $\sigma$ , E and C are computed. These values are compared with the values given in Table 1. If the computed values of  $\bar{x}$ ,  $\sigma$ , E and C lie in the range, then it is assumed that the input slice contains the hippocampus and considered for segmentation, otherwise it is discarded.

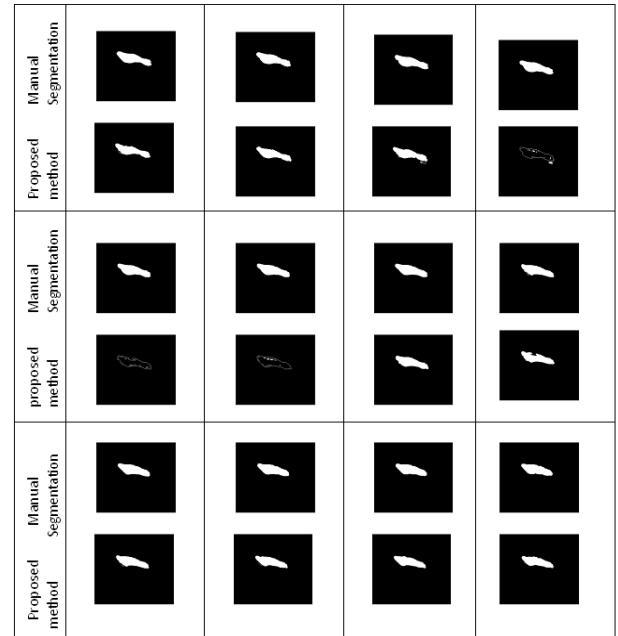


(a)

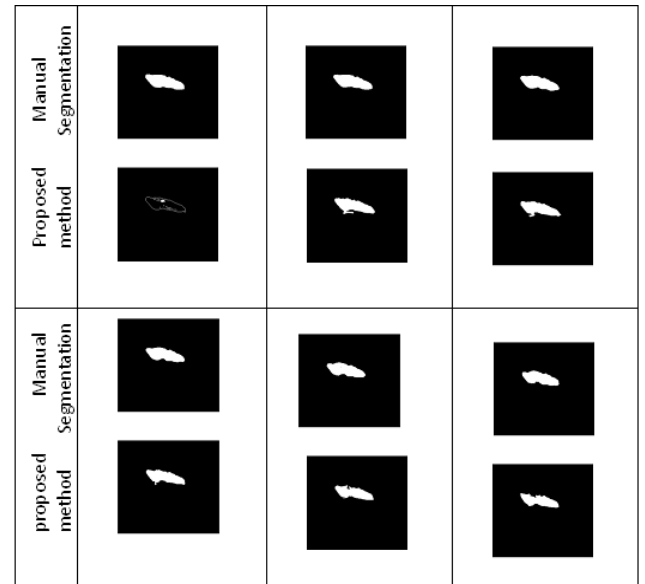
The proposed method proceeds with the segmentation process with the valid input slice. From the previous analysis, the region of interest(ROI), hippocampus is found to lie in the boundary formed with row minimum=90, row maximum=130, column minimum=86, and column maximum=195. The maximum intensity difference between the pixels falling within the hippocampus region is found to be 5.

The next step in the segmentation process is fixing the minimal hippocampus in the ROI. This is done by fixing every pixel present in the minimal hippocampus extracted from the Atlas in the respective positions in the input slice. The proposed method then employs the region growing technique based on intensity difference among the neighborhood pixels, with the boundary cells of this minimal hippocampus as the input. The boundary pixels are found using Sobel edge detection method. The Sobel method finds edges using the Sobel approximation to the derivative. It returns edges at those points where the gradient of the image is maximum. For every pixel present in the edge, the intensity difference between this pixel and the neighborhood pixels are calculated. A maximum intensity difference has been already calculated from the analysis of the post-mortem samples available in the PHA. The neighborhood pixels for which this difference is less than the minimum intensity difference are assumed to be the hippocampus region and added with the fixed minimal hippocampus. After all the boundary pixels are analyzed the hippocampus has grown to the next level. Now the new hippocampus is taken as input for the further process. This boundary pixels detection and neighborhood pixels intensity processes are repeated until a unmatched minimum intensity difference is found. The region growing process stops if this above said condition is satisfied and this is

assumed to be the boundary of the hippocampus. Using the boundary obtained in region growing, the hippocampus is extracted. The segmented hippocampus using the proposed method are shown in Fig 3(a,b,c).



(b)



(c)

Figure 3 (a,b,c) The segmented hippocampus from PHA. In each row the images lying at the top show the manually segmented hippocampus and the images at the bottom are segmented by the proposed

### III. RESULTS AND DISCUSSION

We carried out experiments by applying our method on a stack of 31 slices in left obtained from the data base in PHA which contains 130 slices for 3 right and 2 left hippocampus. The results obtained for the slices containing hippocampus is shown in Fig.3. This set contains hand segmented gold standard. For quantitative analysis we computed the false positive rate(FPR), false negative rate(FNR), sensitivity(S), specificity(Sp), Jaccard

coefficient(J) and Dice coefficient(D) which are calculated as follows.

The Jaccard coefficient(Jaccard, 1912) is given by:

$$J(A, B) = \frac{A \cap B}{A \cup B} \tag{7}$$

where, A and B are two data sets. The value J as well as D varies from 0 for complete disagreement to 1 for complete agreement, between A and B.

Table 2. Performance analysis

S.No.	Slice	Metric						
		Jaccard J	Dice D	Sensitivity S	Specificity Sp	Predictive accuracy PA	FPR	FNR
1	Penn002L_01070	0.7964	0.8866	0.8769	0.9962	99.1845	0.1011	0.1231
4	Penn002L_01073	0.8029	0.8906	0.8481	0.9977	99.1762	0.0563	0.1519
8	Penn002L_01077	0.8697	0.9303	0.8918	0.9988	99.4167	0.0254	0.1082
9	Penn002L_01078	0.8820	0.9373	0.9039	0.9989	99.4667	0.0248	0.0961
10	Penn002L_01079	0.7772	0.8746	0.8155	0.9977	98.9536	0.0492	0.1845
11	Penn002L_01080	0.9047	0.9499	0.9258	0.9989	99.5619	0.0233	0.0742
12	Penn002L_01081	0.8944	0.9442	0.9092	0.9992	99.5131	0.0165	0.0908
13	Penn002L_01082	0.8892	0.9413	0.9102	0.9989	99.4845	0.0236	0.0898
14	Penn002L_01083	0.8720	0.9316	0.8890	0.9991	99.4119	0.0196	0.1110
15	Penn002L_01084	0.8998	0.9472	0.9156	0.9992	99.5440	0.0176	0.0844
16	Penn002L_01085	0.8638	0.9269	0.9016	0.9980	99.3690	0.0437	0.0984
20	Penn002L_01089	0.8929	0.9434	0.9201	0.9986	99.5167	0.0304	0.0799
21	Penn002L_01090	0.8328	0.9087	0.8633	0.9983	99.2405	0.0367	0.1367
22	Penn002L_01091	0.9002	0.9474	0.9268	0.9987	99.5536	0.0296	0.0732
23	Penn002L_01092	0.8908	0.9422	0.9126	0.9989	99.5214	0.0245	0.0874
24	Penn002L_01093	0.9051	0.9501	0.9231	0.9991	99.5905	0.0200	0.0769
25	Penn002L_01094	0.8867	0.9399	0.9083	0.9989	99.5167	0.0243	0.0917
27	Penn002L_01096	0.8637	0.9268	0.9261	0.9969	99.4071	0.0722	0.0739
28	Penn002L_01097	0.8730	0.9321	0.9216	0.9977	99.4607	0.0556	0.0784
29	Penn002L_01098	0.8855	0.9392	0.9175	0.9985	99.5357	0.0362	0.0825
30	Penn002L_01099	0.8743	0.9329	0.8928	0.9991	99.5024	0.0212	0.1072
31	Penn002L_01100	0.8372	0.9113	0.8729	0.9983	99.3643	0.0426	0.1271

The coefficients J and D are related by (Shattuck et al., 2001):

$$D = \frac{2J}{J+1} \tag{9}$$

The quantitative evaluation based on sensitivity (S), specificity (Sp) and predictive accuracy (PA), given in eqns (7), (8) and (9), are performed between the region of interest (ROI) hand – drawn by the experts and the respective portions produced by the proposed methods. These parameters are used to measure the performance of an algorithm against the manual extraction. The sensitivity (S) is the percentage of ROI voxels recognized by an algorithm and specificity (Sp) is the percentage of non-ROI voxels recognized by an algorithm using the True Positive (TP), False Positive (FP), True Negative (TN) and False Negative (FN) values extracted by an algorithm and are given by

$$S = \frac{TP}{TP + FN} \tag{10}$$

$$Sp = \frac{TN}{TN + FP} \tag{11}$$

The predictive accuracy (PA) is the percentage of both ROI and non-ROI regions recognized by the proposed methods. TP and FP are the total number of pixels correctly and incorrectly classified as ROI by the automated algorithm. TN and FN are defined as the total pixels correctly and incorrectly classified as non-ROI tissue by an automated algorithm.

$$PA = 100 \times \frac{TP + TN}{TP + TN + FP + FN} \tag{12}$$

Finally, false positive rate (FPR) and false negative rate (FNR) are used to measure the misclassification done by an algorithm. FPR is the number of voxels incorrectly classified as ROI by the automated algorithm and is given by:

$$FPR = \frac{FP}{TP + FN} \tag{13}$$

The FPR represents the degree of under segmentation and the FNR the degree of over segmentation. The



computed values of J, D, S, Sp, PA, FPR and FNR are given in Table 2.

The proposed automatic method for segmentation of the hippocampus has its own merits and demerits. The performance analysis has revealed that it is comparatively better than the manual segmentation, which is a time consuming process and it needs no human intervention. Our method comparatively requires only the input set selected manually from the MRI volume and no further human intervention is needed.

The average predictive accuracy in shape is 99%. Further work is in progress to implement the same on the real data set for all slices which are obtained from the clinical laboratory containing the images of both the normal and diseased persons and available at Penn Hippocampus Atlas[2].

#### IV. CONCLUSION

In this paper we have proposed an automatic two dimensional segmentation technique for segmenting the hippocampus from the Penn Hippocampus Atlas [2], a resource consisting of segmented and normalized high-resolution postmortem MRI of the human hippocampus. Experimental results show that the proposed method gives satisfactory results. This method also overcomes many of the demerits in the existing methods.

#### V. REFERENCES

- [1] Bruce Fischl, David H. Salat, Evelina Busa, Marilyn Albert, Megan Dieterich, Christian Haselgrove, Andre van der Kouwe, Ron Killiany, David Kennedy, Shuna Klaveness, Albert Montillo, Nikos Makris, Bruce Rosen, and Anders M. Dale, (2002), "Whole Brain Segmentation: Automated Labeling of Neuroanatomical Structures in the Human Brain", *Neuron* vol. 33, pp. 341–355
- [2] MohammadReza Siadat, Hamid Soltanian Zadeh, Kost V. Elisevich, (2007), "Knowledge-based localization of hippocampus in human brain MRI, *Computers in Biology and Medicine* archive, vol. 37, pp. 1342-1360.
- [3] Paul A. Yushkevich, Brian B. Avants, John Pluta, Sandhitsu Das, David Minkoff, Dawn Mechanic-Hamilton, Simon Glynn, Stephen Pickup, Weixia Liu, James C. Gee, Murray Grossman, & John A. Detre (2008), "A high-resolution computational atlas of the human hippocampus from postmortem magnetic resonance imaging at 9.4 T", *Neuroimage* vol.44, pp.385-398.
- [4] Rajendra a. Morey, Christopher M. Petty, Yuan Xu, Jasmeet Pannu Hayes, H. Ryan Wagner II, Darrell V. Lewis, Kevin S. LaBar, Martin Styner & Gregory McCarthy, (2009) "A comparison of automated segmentation and manual tracing for quantifying hippocampal and amygdala volumes", *Neuroimage* vol.45.5, pp.855-866.
- [5] Carmichael O.T., Aizenstein H.A., Davis S.W., Becker J.T., Thompson P.M., Meltzer C.C., & Liu Y., (2005) "Atlas-based hippocampus segmentation in Alzheimer's disease and mild cognitive impairment", *Neuroimage* vol. 27, pp. 979–990.
- [6] Duvernoy, H.M., (2005) "The Human Hippocampus, Functional Anatomy, Vascularization and Serial Sections with MRI", Third ed. Springer.
- [7] Csernansky J.G., Wang, L., Swank J., Miller J.P., Gado M., McKeel D., Miller M.I., Morris J.C., (2005), "Preclinical detection of Alzheimer's disease: hippocampal shape and volume predict dementia onset in the elderly", *Neuroimage* vol.25, pp. 783–792.
- [8] Barnes J., Foster J., Boyes R.G., Pepple T., Moore E.K., Schott, J.M., et al., (2008). "A comparison of methods for the automated calculation of volumes and atrophy rates in the hippocampus". *Neuroimage* vol. 40, pp. 1655–1671.
- [9] McDonald C.R., Hagler D.J., Ahmadi M.E., Tecoma E., Iragui V., Dale A.M., Halgren E., (2008). "Subcortical and cerebellar atrophy in mesial temporal lobe epilepsy revealed by automatic segmentation". *Epilepsy Res.* vol.79, pp.130–138.
- [10] Powell S., Magnotta V.A., Johnson H., Jammalamadaka V.K., Pierson R., Andreasen N.C., (2008). "Registration and machine learning-based automated segmentation of subcortical and cerebellar brain structures", *Neuroimage* vol.39, pp. 238–247.

#### Short Bio Data for the Author

**Somasundaram .K** was born in the year 1953. He received the M.Sc degree in Physics from University of Madras, Chennai, India in 1976, the Post Graduate Diploma in Computer Methods from Madurai Kamaraj University, Madurai, India in 1989 and the Ph.D degree in theoretical Physics from Indian Institute of Science, Bangalore, India in 1984. He is presently the Professor and Head of the Department of Computer Science and Applications, and Head, Computer Centre at Gandhigram Rural Institute, Gandhigram, India. From 1976 to 1989, he was a Professor with the Department of Physics at the same Institute. He was previously a Researcher at an International Centre for Theoretical Physics, Trieste, Italy and a Development Fellow of Commonwealth Universities at the school of Multimedia, Edith Cowan University, Australia. His research interests are in image processing, image compression and medical imaging. He is a Life member of Indian Society for Technical Education and Telemedicine Society of India. He is also an annual member in ACM, USA and IEEE Computer Society, USA.



**Vijayalakshmi .S** was born in the year 1975. She received the B.Sc. degree in Computer Science from Bharathidasan University, Trichirapalli, India in 1995, the MCA degree from the same University in 1998 and the M.phil. degree from the same University in the year 2006. She has been working as an Assistant Professor in Department of Computer Science and Applications, Gandhigram Rural Institute – Deemed University, Gandhigram, Dindigul, TamilNadu, India on adhoc basis from 1998. She is a part time research scholar doing research in Medical Imaging.

